

Thomas Carrel-Billiard ⁽¹⁾, Robin Marty ⁽¹⁾, Louis Rivoire ⁽¹⁾, Philippe Chambon ⁽¹⁾, Nadia Fourrié ⁽¹⁾, Olivier Audouin ⁽¹⁾, Jérôme Vidot ⁽¹⁾, Sophie Djalal ⁽²⁾, Josiane Costeraste ⁽²⁾, Véronique Pascal ⁽²⁾, Joël Michaud ⁽²⁾, Adrien Deschamps ⁽²⁾, Clémence Pierangelo ⁽²⁾, Laura Hermozo ⁽²⁾, Frédéric Bernard ⁽²⁾, Thierry Martin ⁽²⁾, Romain Pinède ⁽²⁾, Laura Le Barbier ⁽²⁾, Elisa Baldi ⁽²⁾ and Citlali Cabrera ⁽³⁾
⁽¹⁾ CNRM, Météo-France and CNRS, Toulouse, France, ⁽²⁾ CNES, Toulouse, France and ⁽³⁾ CapGemini, Toulouse, France

Correspondence to thomas.carrel-billiard@meteo.fr

1. Introduction

The Centre National d'Études Spatiales (CNES) is currently investigating the feasibility of a constellation of small sounders in partnership with the Centre National de Recherches Météorologiques (CNRM). This new program, which was given the name of CMIM (Constellation of Mini sounder for Meteorology), aims at complementing existing constellations and improving short and medium range Numerical Weather Prediction (NWP) by 2030-2035. To achieve this, CMIM aims at densifying temperature and water vapor observations especially in the lower layers of the atmosphere by increasing revisits of Infra-Red (IR) and/or Micro-Wave (MW) instruments. CNRM and CNES with industrial support are currently evaluating the potential impact of CMIM by considering different scenarios: number of satellites, orbits, spectral bandwidth for the instruments... To identify the optimal configuration in terms of performance, CNRM has selected the Observing System Simulation Experiment (OSSE) approach. In this specific framework, the simulated observations are assimilated in a forecast using a 4D-Var system with a 6h update cycle. By comparing the quality of the forecast with and without the simulated CMIM observational data, both the impact on NWP and the optimal constellation configuration can be determined.

2. Construction of a Data Assimilation Framework

An Observing System Simulation Experiment consists of a long, uninterrupted forecast called the nature run (NR), which provides a realistic evolution of the atmosphere considered as truth, and a NWP data assimilation system, which is used to compute the best estimation of the variables of the atmosphere and to produce weather forecasts. The models used in the nature run and in the data assimilation system need to be different to avoid the « identical twin problem » already identified by the scientific community (e.g. Hoffman and Atlas, 2016 [1]).

Parameters of the model	Nature run	Data assimilation and forecasting system
Truncation	TL1798	TL798
Resolution over Europe	About 5 km	About 10 km
Resolution over New-Zealand	About 24 km	About 61 km
Physics package	Tiedtke convection scheme	Bougeault convection scheme
Period of study	July to October and November to February (one month of spin-up)	August to October and December to February

Table 1. Parameter Comparison between the Nature Run and the Data Assimilation System

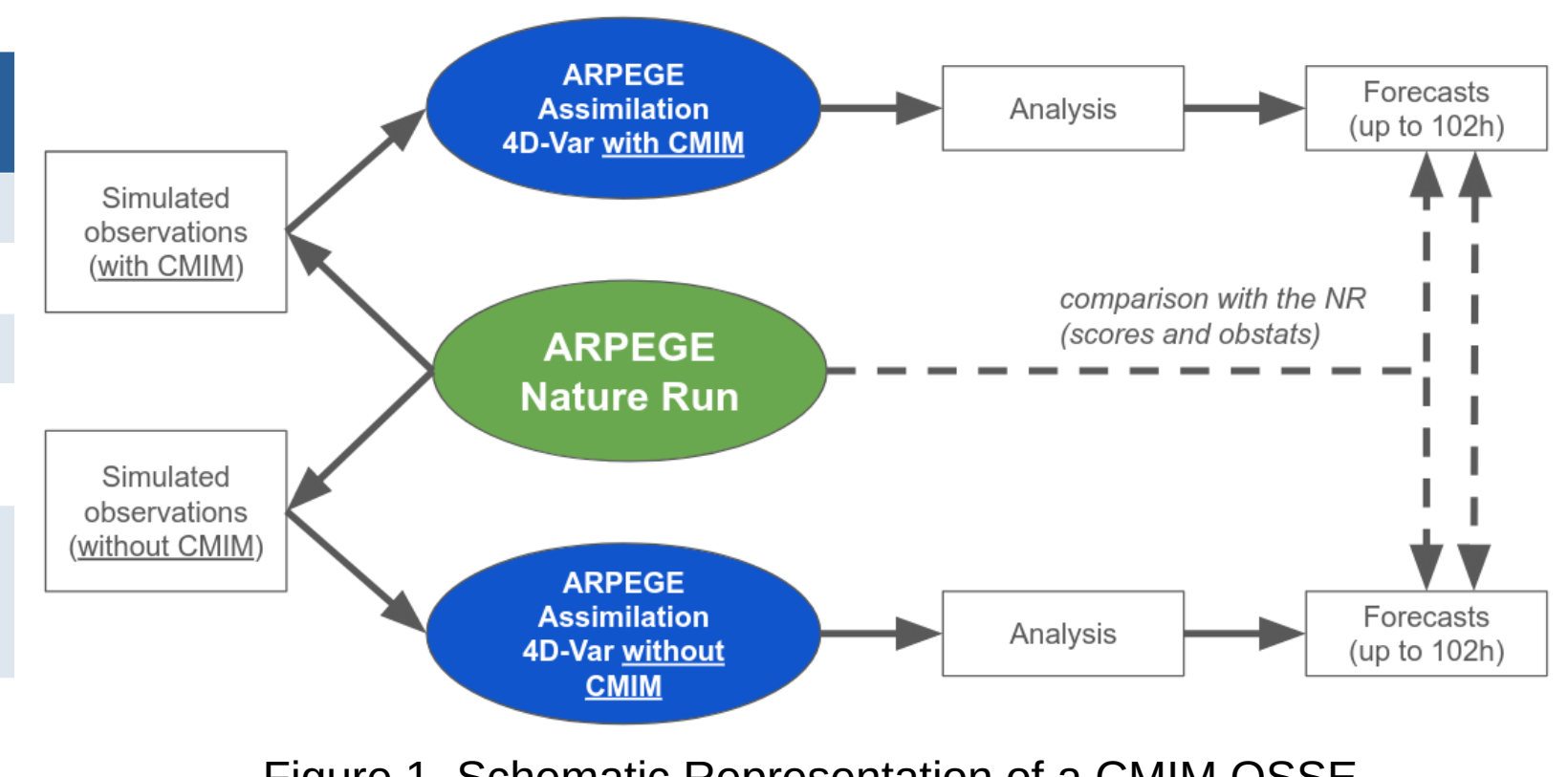


Figure 1. Schematic Representation of a CMIM OSSE

3. Computation and Validation of the Nature Run

The nature run has been computed over the two periods of study. It has then been validated by comparing climatological averages of various variables (temperature, relative humidity) from the nature run and from a real atmospheric analysis. For more details, see the poster of Marty et al.



Scan the QR code to display a video of the evolution of the simulated atmosphere in the nature run in August and September

4. Simulation and Calibration of the Observations

The objective of the study is to measure the impact of the CMIM constellation in a 2030-like environment. Thus, the choice of the observations to simulate is made according to the available information on the planned missions for 2030 and the available proxies in the 2021 observing system. Moreover, the observations are simulated using the NR values and perturbations are added to represent measurements errors. These perturbations have been iteratively calibrated to ensure that each observing system is given a realistic weight within the OSSE. For more details, see the poster of Rivoire et al.

5. Reference Scenarios for CMIM

To determine the CMIM configuration that will have the most favourable impact on the NWP, several scenarios have been or will be studied. Out of those scenarios, two have been selected alongside with the CNES to serve as references: one IR configuration and one MW configuration.

Infra-Red (IR) Reference CMIM Scenario

- The IR reference scenario will consist of:
 - 8 sun-synchronous orbits at 630km of altitude
 - 2 satellites per orbital plane, expected revisit period: 3h30
 - Swath size of 1,100km
 - Horizontal resolution of 3km
 - 2 spectral bands: B1 = [645, 800]cm⁻¹ and B2 = [1200, 1550]cm⁻¹
 - Spectral sampling 0.9cm⁻¹, Spectral resolution: 2 x IASI
 - Horizontal sampling 30x30km
 - NEAT(CMIM-IR) = 3 x NEAT(IASI)

Micro-Wave (MW) Reference CMIM Scenario

- The MW reference scenario will consist of:
 - 8 sun-synchronous orbits at 630km of altitude
 - 2 satellites per orbital plane, expected revisit period: 3h30
 - Swath size of 1,246km
 - Horizontal resolution of 7km
 - 6 high-frequency humidity channels (see table below)
 - SAPHIR-like scenario

Channel Number	Frequency [GHz]	Bandwidth [MHz]	Noise [K]
1	183.31 +/- 0.2	200	1.6
2	183.31 +/- 1.1	350	1.2
3	183.31 +/- 2.7	500	1.0
4	183.31 +/- 4.2	700	0.9
5	183.31 +/- 6.6	1,200	0.7
6	183.31 +/- 11.0	2,000	0.5

Table 2. Channel List for the CMIM MW Reference Scenario

Other IR scenarios have been computed. First, the impact of a spectral bandwidth reduction has been assessed. Such reduction could diminish the size of the IR instrument to be embarked. Then, the orbit sampling precision has been tested, to determine if impacts on NWP are tightly linked to the initial number of observation points to be processed. Results of those studies can be found in section 8. Other scenarios to be tested are presented in section 10.

On the MW side, an alternative scenario has been carried out where the NEAT of the channels (i.e. the noise values from Table 2) have been divided by 3 to simulate a superobbing using 3x3 pixels. Preliminary results are presented in section 9.

6. Integration of the CMIM Constellation

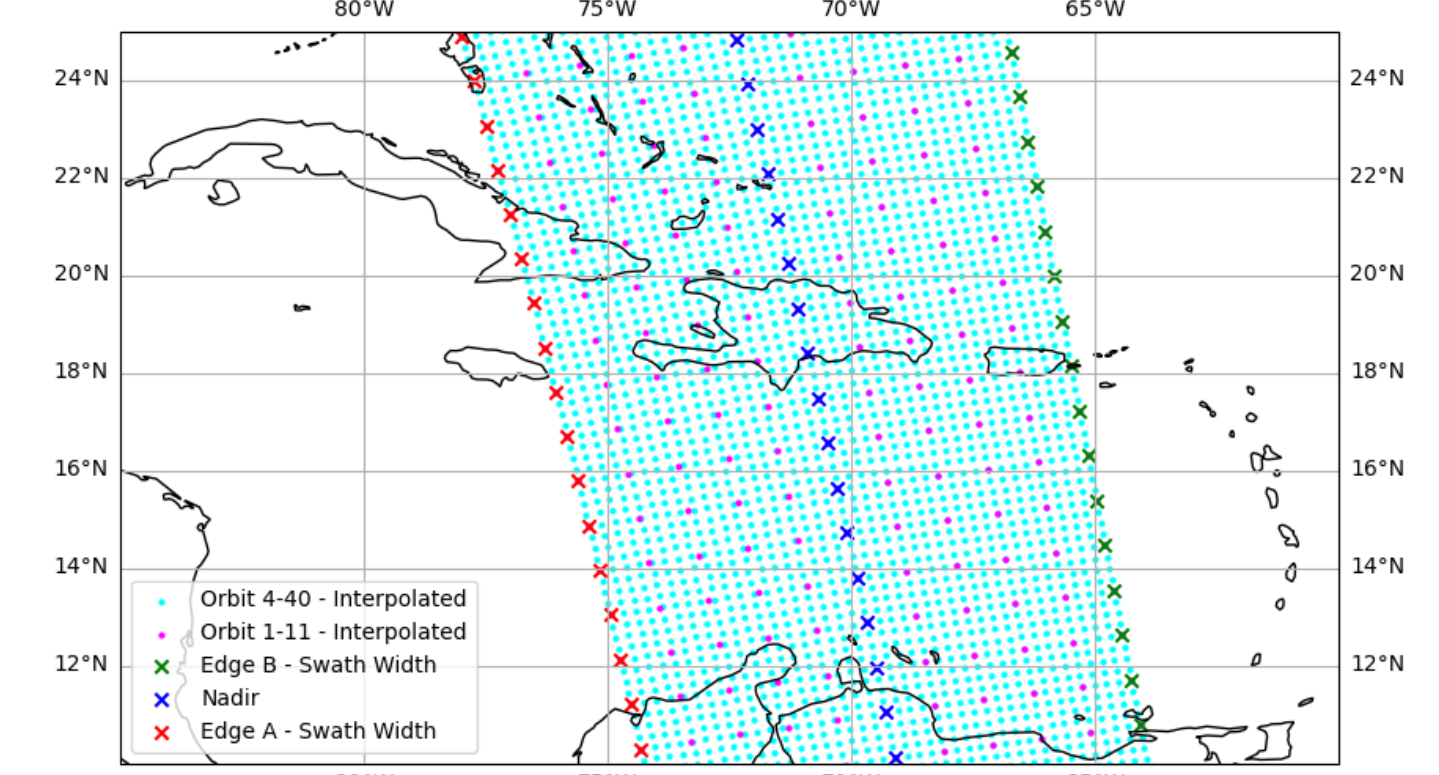


Figure 2. Interpolated CMIM Orbit #1 - Above the Caribbean Sea

The integration has been split in 2 parts, the IR and the MW integration.

CMIM-IR Integration

For the CMIM-IR the first part was (A) to establish the orbit sampling from the ephemerides provided by CNES. Sampled points are obtained through linear interpolation both across a swath width and between two swaths. As seen from Figure 2, the reference IR scenario uses a 4-40 orbit, with corresponds to a 30 by 30km horizontal sampling.

Next, (B) the radiative transfer coefficients were obtained using RTTOV v12 for both clear sky and all-sky conditions. Those coefficients were provided by the Centre d'Études en Météorologie Satellitaire (CEMS).

Afterwards, investigations were carried (C) to determine the channels to be assimilated. For the channel selection, the 129 assimilated IASI channels were chosen as the starting point. Using the CMIM-IR spectral range and the spectral sampling, the IASI channels were mapped to obtain 93 corresponding channels. In order to sample the entire atmosphere both in temperature and humidity, 20 channels were added taken into account their weight functions, resulting in 113 channels to be assimilated. Figures 3 and 4 show the channels that are assimilated everywhere and those assimilated on sea only. The threshold for such distinction was taken to be 800 hPa.

The process described above also allowed to list 200 channels for the (D) configuration of the cloud-detect algorithm. This algorithm based on the work of McNally and Watt [2] identifies the cloud's characteristic signal from the discrepancies between clear-sky simulated radiances and all-sky observed radiances. Channels affected by the clouds are rejected from the assimilation process.

Finally the last step was to (E) compute the covariance matrix for observational errors, know as the R matrix, using the Desroziers [3] methodology.

This matrix was obtained through an iterative process. It can be seen from Figure 5 on the right that the strongest correlations lie in the water vapour region between 1,330 and 1,400cm⁻¹. Moreover, strong correlations also exist for the surface channels around 750cm⁻¹. Both behaviours have also been identified in IASI's R matrix [4].

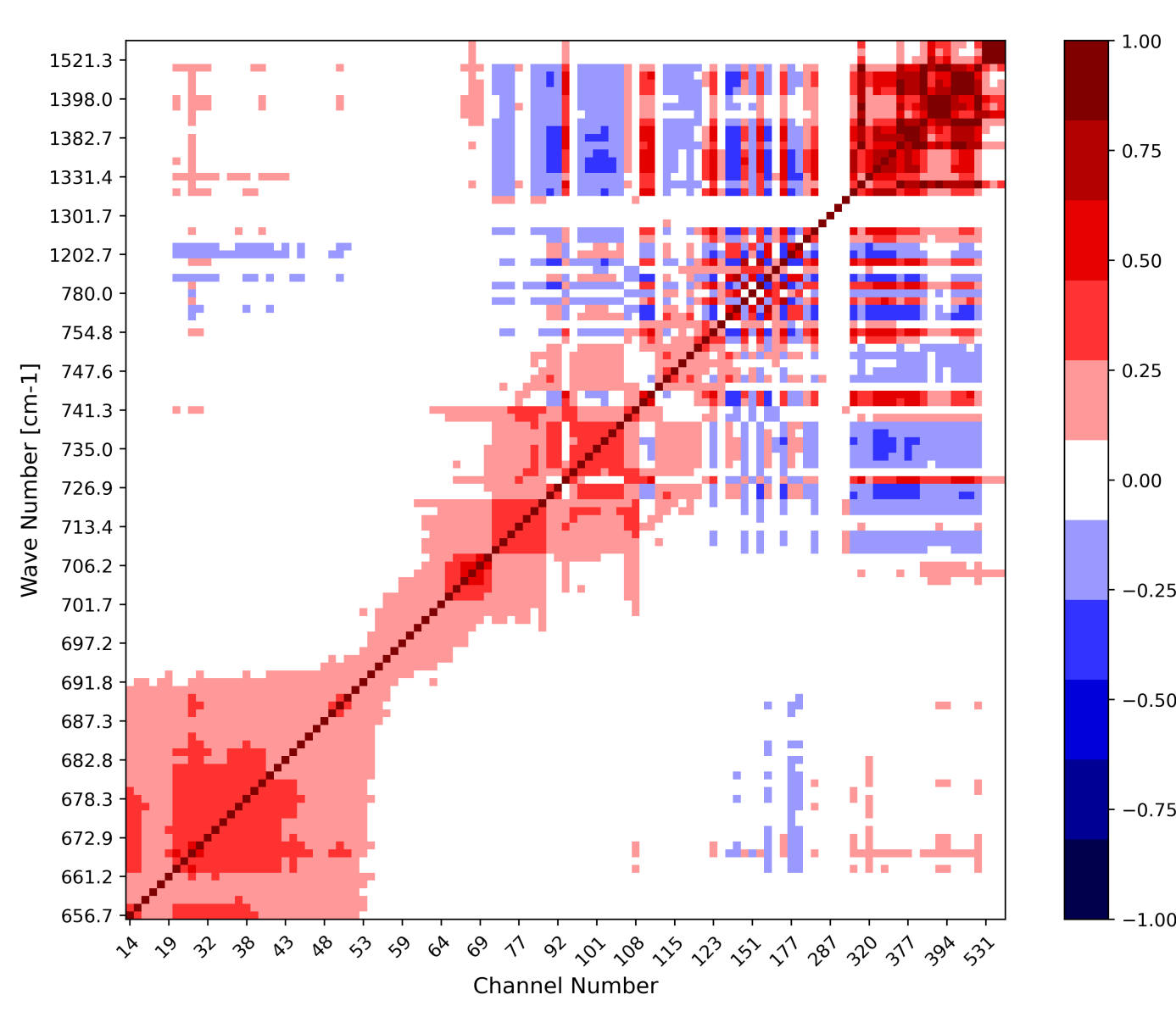


Figure 5. Observational Error Covariance Matrix for CMIM-IR

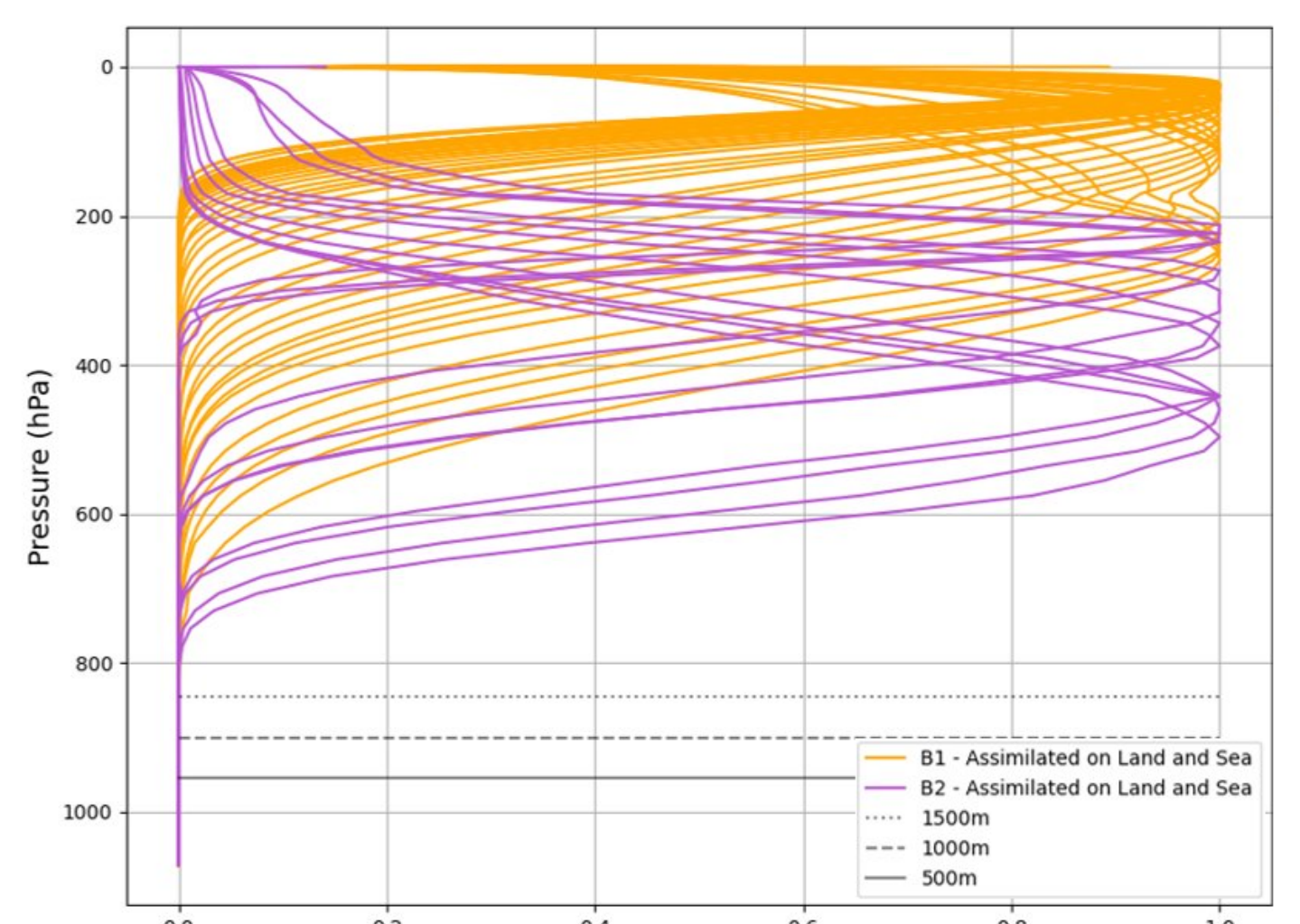


Figure 3. Weight Functions for CMIM-IR Channels assimilated on Land and Sea, 58 channels

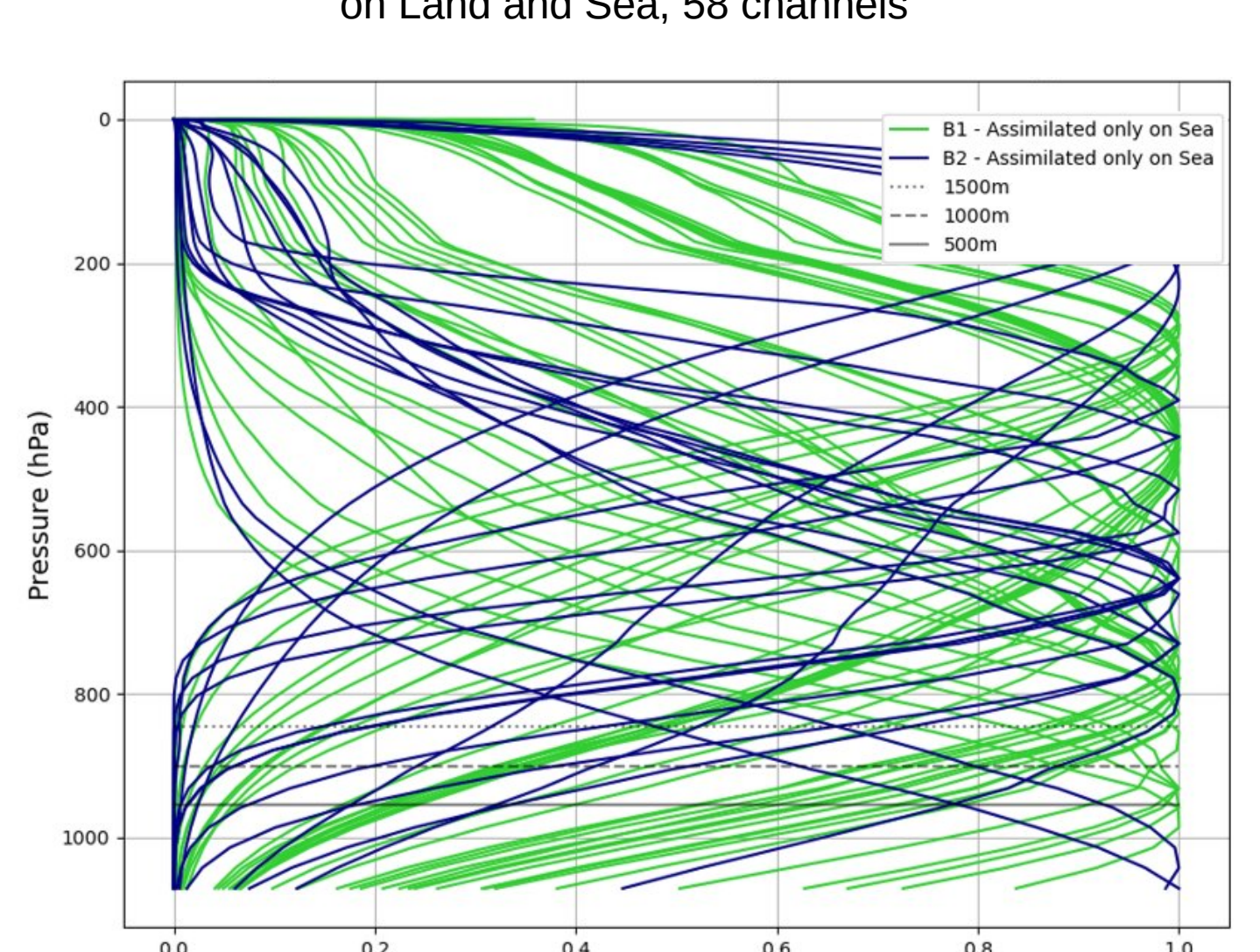


Figure 4. Weight Functions for CMIM-IR Channels assimilated on Sea only, 55 channels

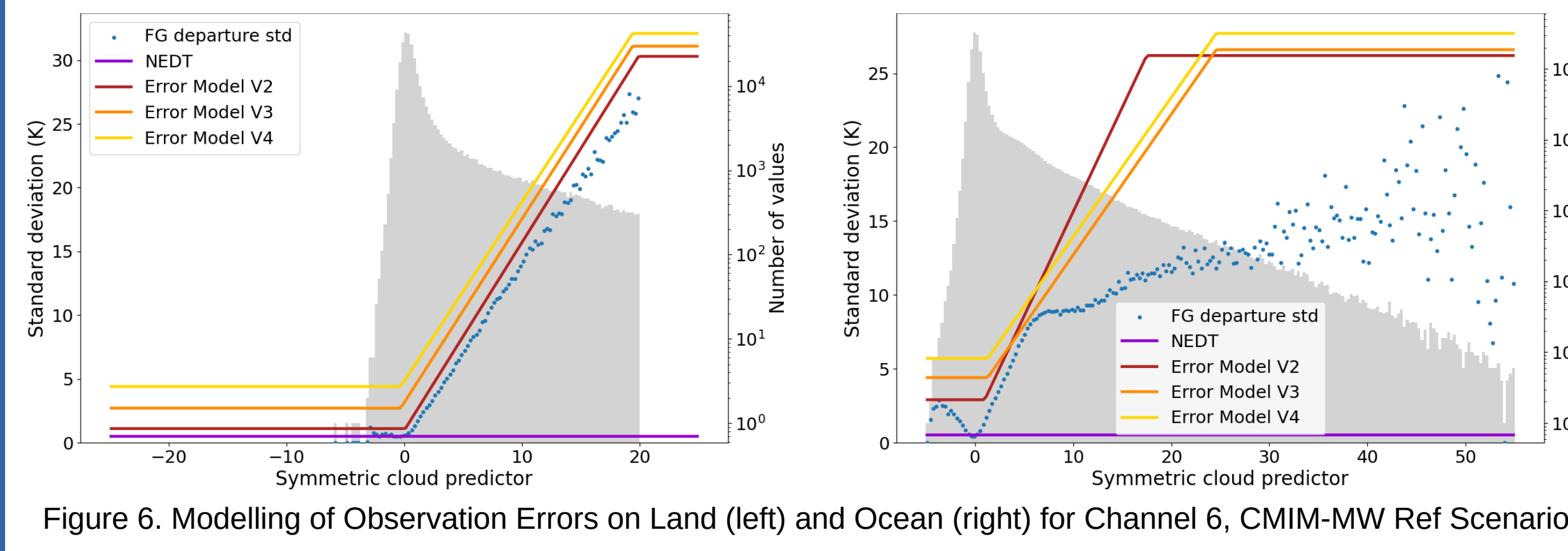


Figure 6. Modelling of Observation Errors on Land (left) and Ocean (right) for Channel 6, CMIM-MW Ref Scenario

CMIM-MW Integration

The observations from CMIM-MW are assimilated in all-sky conditions, over oceans and land using the all-sky approach developed at the European Centre for Medium-Range Weather Forecasts (ECMWF). The error models for CMIM-MW are constructed by fitting the standard deviations of first-guess departures. Examples are given in Figure 6 with a symmetric cloud predictor both on land and on ocean.

7. Impact of CMIM-IR - The Reference CMIM-IR Scenario

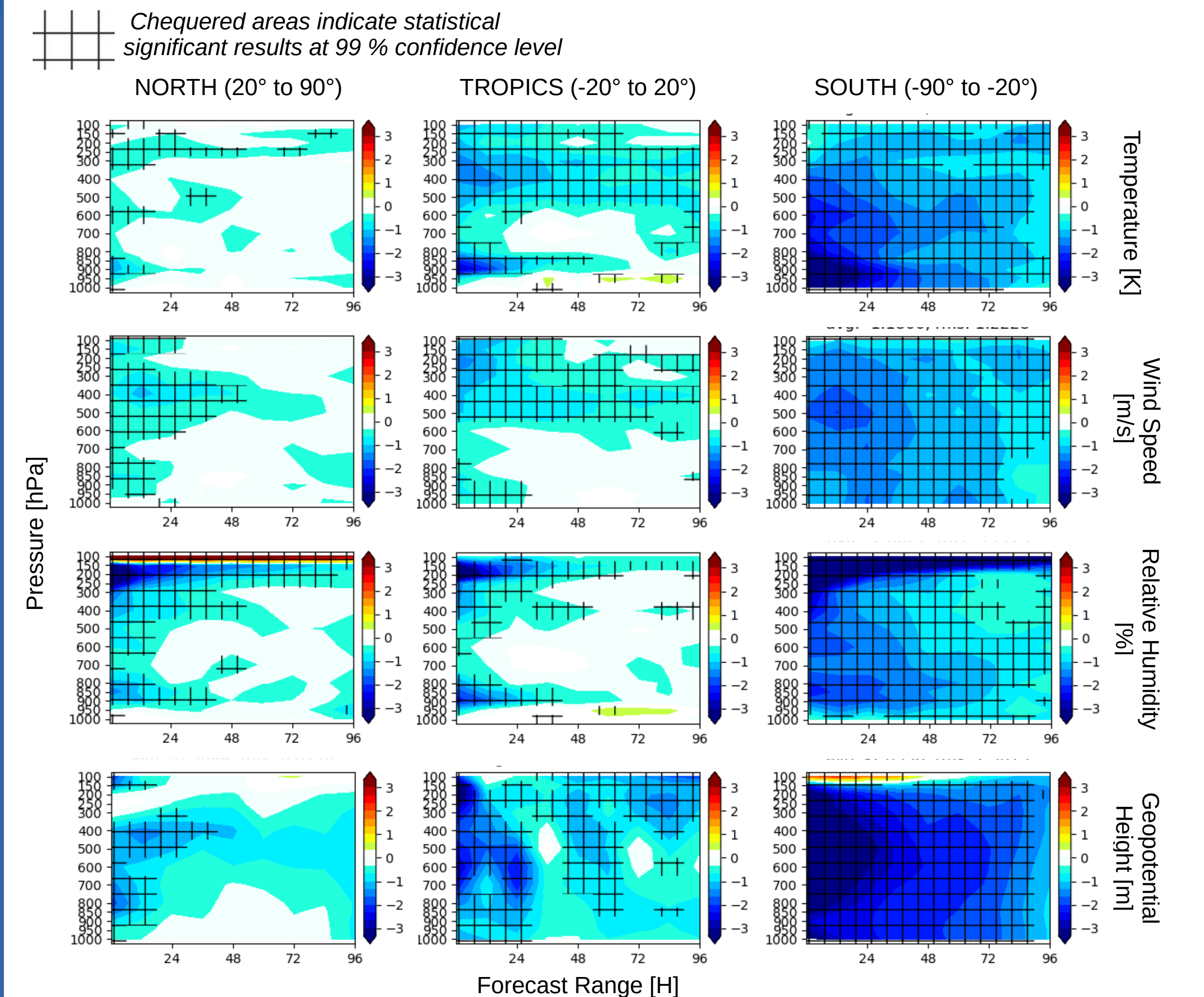


Figure 7. Relative impact of the CMIM-IR reference scenario on forecast errors (%) - 2 months (from 14/08/2021 to 13/10/2021) - North (20° to 90°), Tropics (-20° to 20°) and South (-66° to -20°)

Figure 7 demonstrates that all geographic zones are positively impacted by the CMIM-IR reference configuration. On the entire Globe, the relative improvements for the NWP vary from 0.7 to 1.3%. The improvements are the strongest in the South region where there are less conventional observations. This is also confirmed by Figure 8 below.

Moreover, in the Southern Hemisphere, the positive impact is significant up to +96h for all variables except for the relative humidity where there is a lack of significance beyond 72h between 200 and 500hPa.

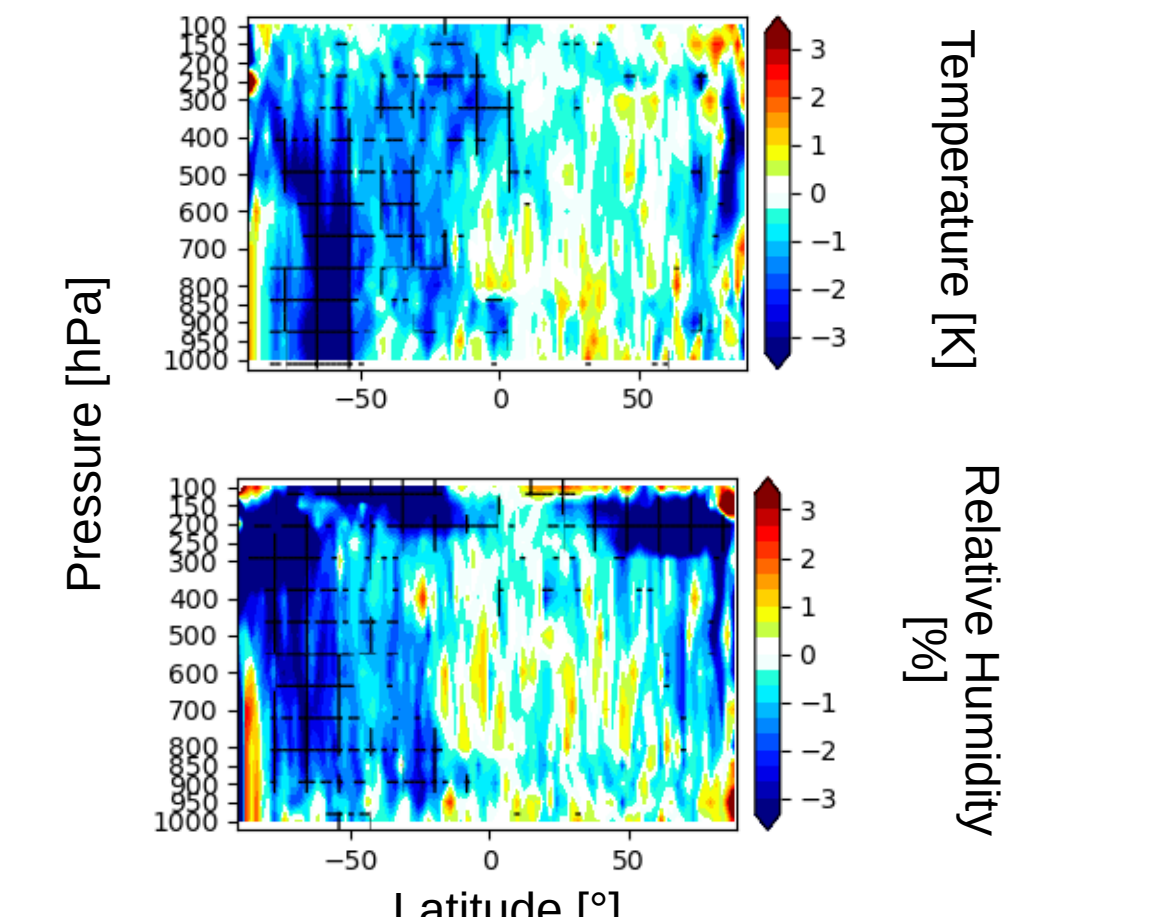


Figure 8. Relative impact of the CMIM-IR reference scenario on forecast errors (%) - Forecast Range 24h - 2 months (from 14/08/2021 to 13/10/2021) - Zonal STD

8. Impact of CMIM-IR - The Effects of Bandwidth Reduction and Orbit Sampling

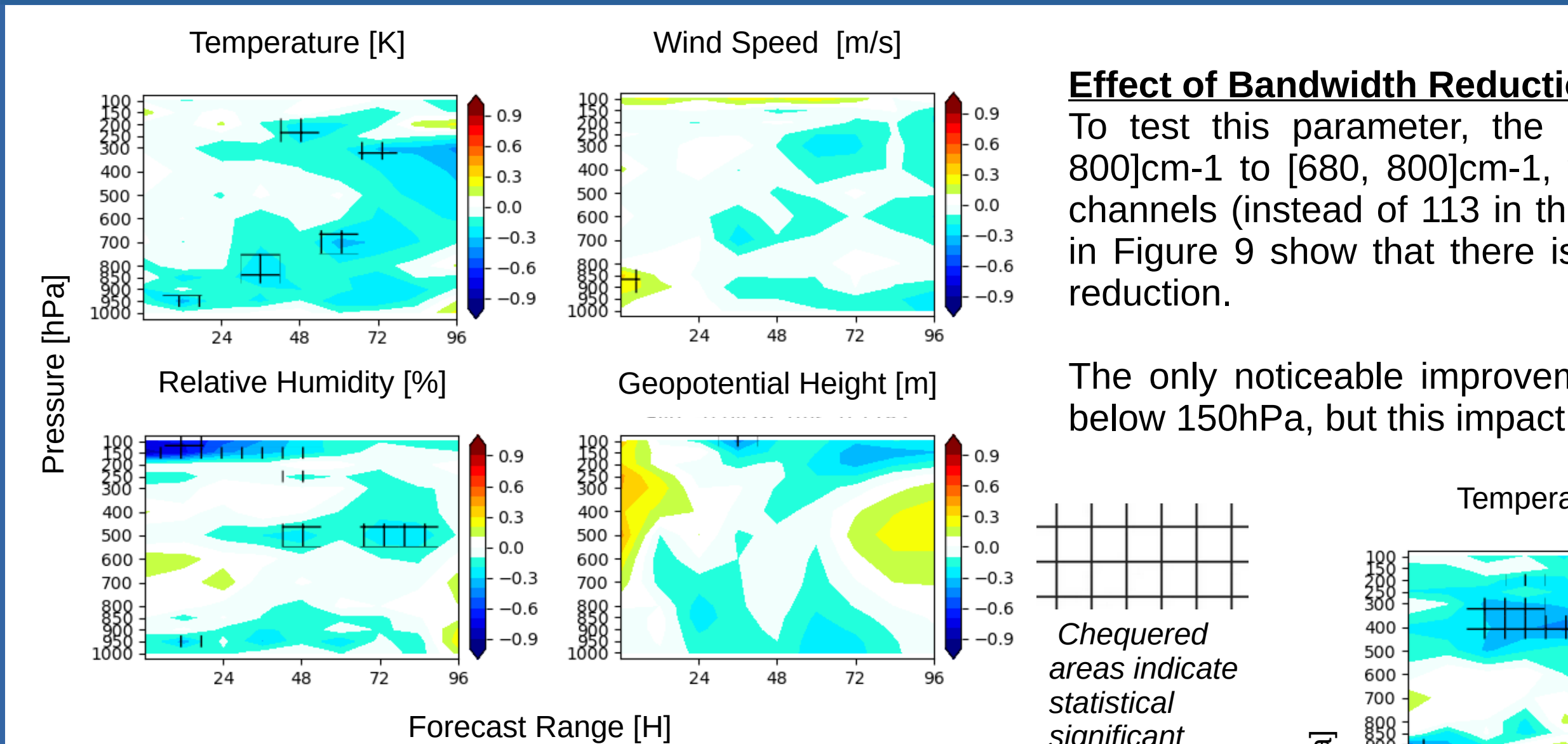


Figure 9. Relative impact of the CMIM-IR reduced bandwidth scenario as compared to the CMIM-IR reference scenario - 2 months (from 14/08/2021 to 13/10/2021) - Globe

Effect of Bandwidth Reduction

To test this parameter, the B1 spectral band was reduced from [645, 800]cm⁻¹ to [680, 800]cm⁻¹, which corresponds to the assimilation of 96 channels (instead of 113 in the reference configuration). Results displayed in Figure 9 show that there is little to no degradation with this bandwidth reduction.

The only noticeable improvement can be seen for the Relative Humidity, below 150hPa, but this impact is only short-term (before 24h).

Effect of Orbit Sampling

To study this parameter, a 5-56 orbit was generated (56 interpolated points across a single swath width and 5 interpolated points between two swaths), resulting in a 20x20km horizontal sampling. This reduction in sampling was computationally expensive as it more than doubled the number of observational points to be processed. As expected, Figure 10 does show some improvements in reducing the horizontal sampling but the results are not significant enough to justify the extra computing resources required.

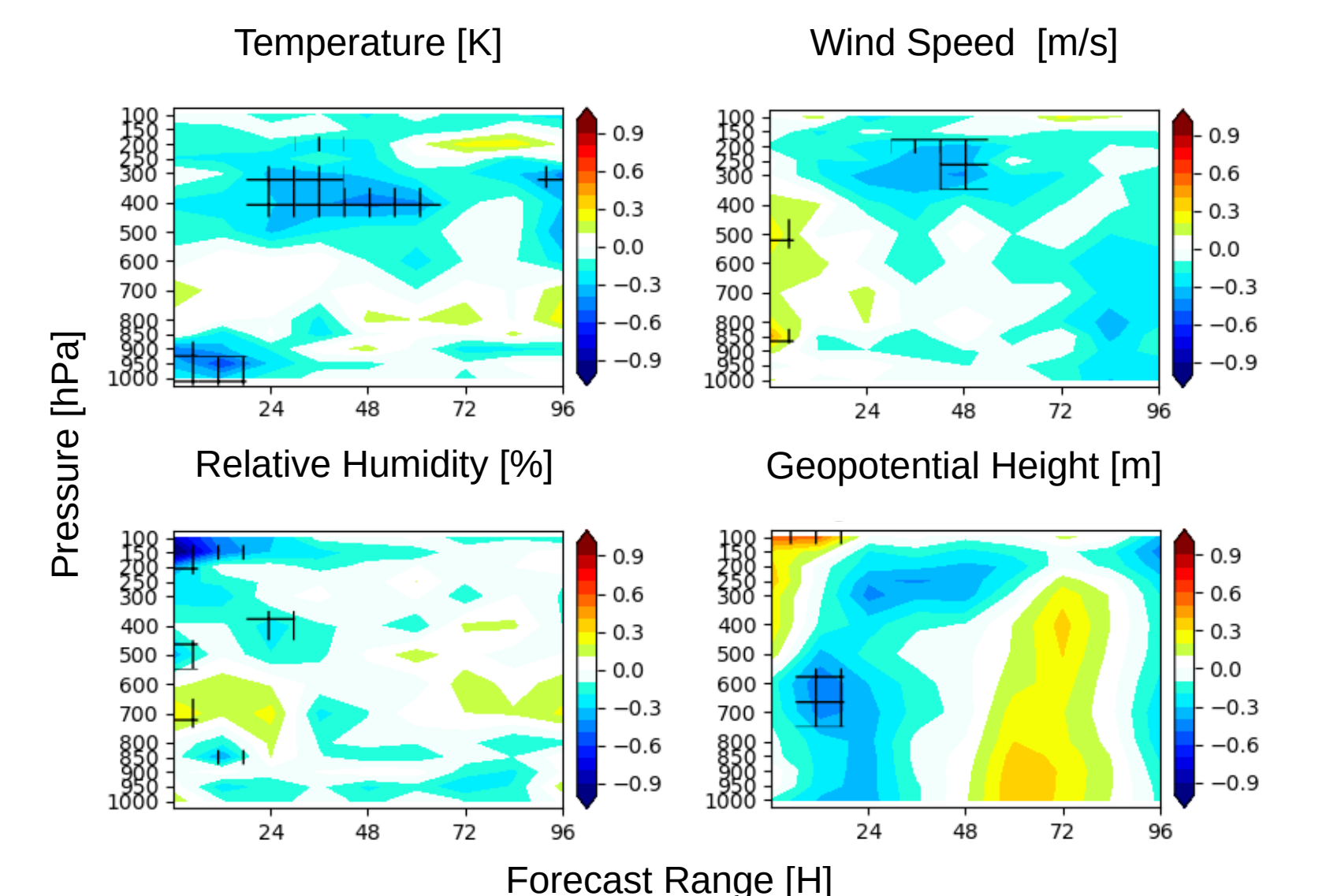


Figure 10. Relative impact of the CMIM-IR 20x20km orbit sampling as compared to the CMIM-IR reference 30x30km sampling - 1 month (from 14/08/2021 to 13/09/2021) - Globe

9. Impact of CMIM-MW - Preliminary Results

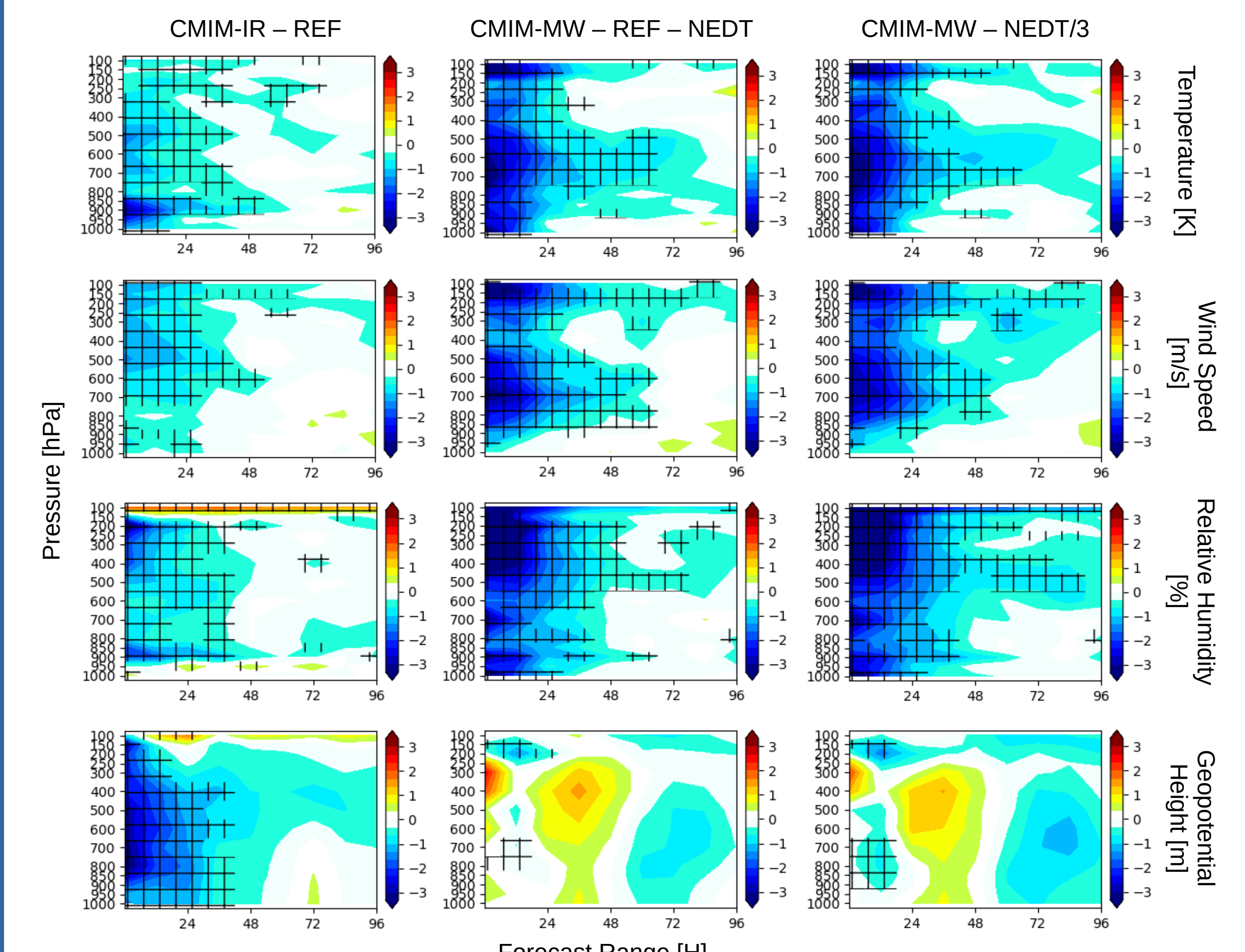


Figure 11. Relative impact of the multiple CMIM scenarios on forecast errors (%) - 9 days (from 15/08/2021 to 23/10/2021) - Globe

The CMIM-MW preliminary results were obtained thanks to observation model V4 presented in Figure 6 (yellow curve).

For the first 9 days of OSSE and over the Globe, the CMIM-MW reference scenario already shows positive impact on the NWP on short term forecast (<24h) for Temperature, Wind Speed and Relative Humidity. This positive impact affects all pressure layers. For the Geopotential height, a degradation is observed between 200 and 500hPa. This behaviour could come from Channel 6 that is both used for the construction of the cloud predictor (Figure 6) and assimilated in the OSSE.

Dividing the NEAT of the channels by 3 to simulate a superobbing does seem to slightly improve results.

Moreover, when comparing with the CMIM-IR reference scenario, the CMIM-MW reference scenario already seems to have a more beneficial impact. However those are only preliminary results which need to be consolidated.

10. Conclusions and Future Work

The results presented demonstrate that the reference CMIM-IR configuration has a positive impact on the NWP, improving it between 0.7 and 1.3% across the Globe. Both the bandwidth reduction and the reduction of the orbit sampling do not show significant impact as compared to the reference scenario. For the CMIM-MW reference scenario, the first results are promising but need to be consolidated. It should be noted that the framework built for this OSSE suffers from several limitations that are described in the poster of Rivoire et al.

In the coming months, the following tasks will be addressed:

- Consolidation of the results for the CMIM-MW high-frequency reference scenario
- Other parameters that could affect the NWP will be tested. For IR: the impact of revisit period, and the increase of the NEAT. For MW: a low-frequency scenario. Moreover, a combination of both instruments will be tested as well as a IRS-like scenario (CMIM as a GEO). The objective of this latter scenario is to determine the impact of MTG in the 2030 observing system.

11. References

- Hoffman, R. N., & Atlas, R. (2016). Future Observing System Simulation Experiments. Bulletin of the American Meteorological Society, 97(9), 1601-1616.
- McNally, A.P. and Watts, P.D. (2003). A cloud detection algorithm for high-spectral-resolution infrared sounders. Q.J.R. Meteorol. Soc., 129: 3411-3423.
- Desroziers, G., Berre, L., Chapnik, B. and Poli, P. (2005). Diagnosis of observation, background and analysis-error statistics in observation space. Q.J.R. Meteorol. Soc., 131: 3385-3396.
- Stewart, L. M., Dance, S. L., Nichols, N. K., Eyre, J. R. and Cameron, J. (2014). Estimating interchannel observation error correlations for IASI radiance data in the Met Office system. Quarterly Journal of the Royal Meteorological Society, 140 (681), pp. 12361244.